

Article

Removal of Contaminants in Water with Scallop Shell Waste

Pablo Zavala Sore ¹, Adriana C. Mera ², Armando Díaz Concepción ³, José Luis Valin Rivera ⁴,
Meylí Valin Fernández ⁵, Carlos Arturo Navarrete Rojas ⁶ and Alexander Alfonso-Alvarez ^{1,*}

- ¹ Departamento de Ingeniería Mecánica, Facultad de Ingeniería, Universidad de La Serena, Benavente 980, La Serena 1700000, Chile; pzavalasore@hotmail.com
- ² Instituto Multidisciplinario de Investigación y Postgrado (IMIP), Universidad de La Serena, Raúl Bitrán 1305, La Serena 1700000, Chile; amera@userena.cl
- ³ Centro de Estudios de Ingeniería de Mantenimiento, Universidad Tecnológica de La Habana, La Habana 19390, Cuba; adiaz@mecanica.cujae.edu.cu
- ⁴ Escuela de Ingeniería Mecánica, Pontificia Universidad Católica de Valparaíso, Valparaíso 2340025, Chile; jose.valin@pucv.cl
- ⁵ Department of Mechanical Engineering (DIM), Faculty of Engineering (FI), University of Concepción, Concepción 4030000, Chile; mvalin@udec.cl
- ⁶ Departamento de Matemáticas, Facultad de Ciencias, Universidad de La Serena, Benavente 980, La Serena 1700000, Chile; cnavarrete@userena.cl
- * Correspondence: alexander.alfonso@userena.cl

Abstract: Currently, the cultivation and harvesting of mollusks is a crucial activity worldwide. However, this industry generates a large amount of mollusk shell waste disposed of in landfills, causing environmental pollution. In addition, the companies linked to this item allocate large sums of money to depositing the shells in authorized landfills. In South America, Chile is one of the leading producers worldwide of scallop shell (*Argopecten purpuratus*) waste, creating a growing environmental and financial problem in the country, especially considering that there has yet to be progress in the development of new technologies that may reuse this waste in Chile. This study used different techniques to completely characterize the northern Chile scallop shell waste's physical and chemical properties for the first time. The XRD result corresponded with calcite crystal structures (CaCO₃), and the XFR showed 97.68% purity. Three particle sizes were obtained: BS (595–100 μm), MS (250–595 μm), and SS (<250 μm). In addition, the potential use of these wastes to remove contaminants present in water from the wine industry (caffeic acid) and some drinking water (arsenic(III)) was evaluated. The powder with the smallest particle size (SS), which has a surface area of 1 m²/g, 0.0050 m³/g of pore volume and pore diameter of 18.0 nm, removed 100.0% of CA and 23.0% As(III) in a pH condition of 4.6. The results show that scallop shell waste can be used to treat water and reinforce polymeric matrix composite materials to improve mechanical properties.

Keywords: scallop shells; wastes; caffeic acid; arsenic(III); water contamination



Citation: Sore, P.Z.; Mera, A.C.; Concepción, A.D.; Rivera, J.L.V.; Valin Fernández, M.; Navarrete Rojas, C.A.; Alfonso-Alvarez, A. Removal of Contaminants in Water with Scallop Shell Waste. *Appl. Sci.* **2024**, *14*, 3499. <https://doi.org/10.3390/app14083499>

Academic Editor: María Emma Borges

Received: 19 February 2024

Revised: 9 April 2024

Accepted: 17 April 2024

Published: 21 April 2024



Copyright: © 2024 by the authors. Licensee MDPI, Basel, Switzerland. This article is an open access article distributed under the terms and conditions of the Creative Commons Attribution (CC BY) license (<https://creativecommons.org/licenses/by/4.0/>).

1. Introduction

Since the 1950s, global production from the fishing and aquaculture industry has increased from 19 to 179 million tonnes by 2018, where at least 22 million were intended for non-food uses like fishmeal and fish oil. Also, consumption is expected to increase by 15% by 2030 [1]. This significant increase in consumption has generated a large amount of waste, such as bones, scales, and shells. The shells, for their part, can constitute up to 75% of the weight of the mollusk [2], being one of the wastes that the fishing and aquaculture industry generates the most, which in 2018 represented 16% of this industry's total production [3].

Mussels have had the greatest increase in production in the aquaculture industry, followed by oysters, scallops, and pectens, among others [4]. However, the shells of those mollusks have been dumped at sea or sent to landfill, leaving piles of shells through the years where, at the moment, decomposition of the shells is carried out via special

treatments, like thermal decomposition or incineration that requires temperatures higher than 1000 °C [5]. Nowadays, the term blue economy is a concept that seeks a sustainable utilization of marine resources, beginning with the correct valorization of shell waste [6]. For that reason, many strategies of mollusk shell waste management and reutilization have been proposed in different fields such as environmental applications, food and feed additives, biomaterials, and construction [7].

In the case of Chile, the production of mollusks reached 406 thousand tons in 2020, the country with the third highest production in the world [1]. Among the most frequently farmed mollusks are the mussel (*Mytilus chilensis*), choro (*Choromytilus chorus*), cholla (*Aulacomya ater*), Chilean oysters (*O. chilensis*), Pacific oysters (*C. gigas*), and the northern oyster or scallop (*Argopecten purpuratus*) [8]. The latter is distributed from the coasts of Nicaragua to the city of Valparaíso in Chile, but it is located mostly between the first and the fourth region of Chile because the geography of these places benefits their growth. In recent decades, this resource has seen a great demand, which is why various artificial crops have been placed on the shores of those regions to sustain the commercial activity [9].

At the moment, northern scallop production in Chile is concentrated in just a third of the companies founded at the beginning of this industry, and the industry is focused on production volumes with the main challenge being to develop technology to reduce production costs [10]. The Coquimbo region (IV region, Chile) has 93.9% of the national production of northern scallops, which was 3654 tons in 2021 [11]. This mollusk is in great demand due to its high nutritional value, being a good source of tryptophan, vitamin B12, minerals, and an interesting amount of omega-3 fatty acids (EPA and DHA). It is mainly exported, without shells or with only one of them, to countries such as France (87% of the volume exported), Italy (6.7%), and Spain (3.3%) [12].

Consequently, this causes a large amount of shell waste in the region after the cleaning and packaging process to be sold abroad. Therefore, scallop shells have become a problem for artisanal fishermen and the region's companies, who must pay thousands of dollars (USD) annually to transport and dispose of the residue in authorized landfills. In addition, a single company generates approximately 1000 tons of shells per year as waste, ending in landfills and creating severe environmental problems. Over time, they decompose, producing foul odors, contaminating the soil and the environment, and releasing toxic gases such as NH₃ and H₂S [13]. These are just some of the reasons fisheries and aquaculture are among the UN Sustainable Development Goals (SDGs), making it necessary to have policies and actions promoting a circular economy and sustainable development [14].

Seashells are a composite biomaterial made up of 95–99% calcium carbonate (CaCO₃), with different superimposed CaCO₃ layers, which are microstructures of calcite or aragonite, and an external organic layer [15]. Since prehistoric times, seashells have been used by many cultures as tools, ornaments, and artifacts [16]. Also, some of those developed a currency based on seashells that facilitated trade, the purchase of food, and payment for services [17]. Currently, they have different applications, such as being used in additives for construction materials [18,19], construction of rural roads [20], animal feed supplements [6], lime for industrial sectors [21], and additives for agricultural soils [22].

Other studies have found that the shell waste possesses antifungal properties [23]; in agriculture, they can prevent the loss of soil nutrients by leaching [24] and reduce the accumulation of Cd in plantations of brown rice, oilseeds, and radishes [25,26]; in contaminated mining soils, calcined shell waste can decrease the concentrations of Cd and Pb [27,28]. Also, shell waste subjected to pyrolysis can eliminate 98% of phosphates in wastewater [29], and adhering them to filtering processes can increase the removal efficiency of COD, NH₃-N, and phosphorus [30], remove methylene blue [31] and stabilize or precipitate heavy metals in water, such as arsenic, nickel, and copper [32,33]. These are some of the uses that are given to mollusk shell waste as a resource in another process or product, promoting the circular economy.

This work describes the physical and chemical properties of the northern Chile scallop shell, specifically those produced in the Coquimbo region, which had not been previously

reported in the literature. Such properties provide key information when defining possible applications for this waste in different fields. Out of these possibilities, this study proposes the application of scallop shell waste in water treatment processes, specifically the removal of caffeic acid from wine distillery wastewater as well as the removal of arsenic III ions from certain potable waters. Additionally, the correlation between pore size distribution and water pH was evaluated in order to determine removal percentages of the selected contaminants, which has yet to be reported in the literature.

2. Materials and Methods

2.1. Cleaning, Drying, Grinding and Sieving

The scallop shells from northern Chile were obtained in the IV region from a company in the sector dedicated to farming, processes, harvesting, and marketing of this mollusk. This shell waste was, in a first stage, washed to remove residues present such as sand and organic materials. The washing process was carried out in a large enough container to ensure a good distribution of the scallop shell waste; these were submerged in a sodium hydroxide (NaOH, 97%, WINKLER, Santiago, Chile) solution at 4% for 24 h [34]. After, the scallop shells were removed from this solution and were rinsed three times with abundant distilled water (A, see Figure 1).

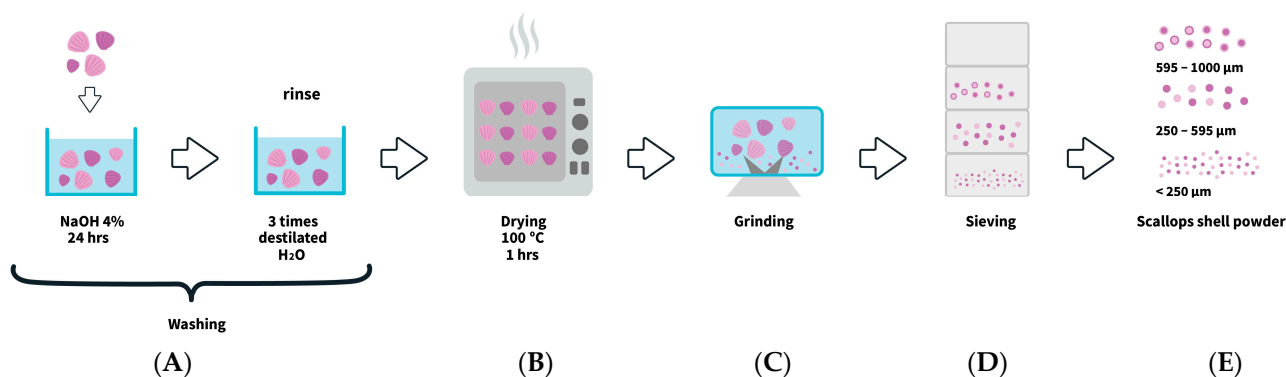


Figure 1. Washing (A); drying (B); grinding (C); sieving of scallop shell waste (D); particle size classification (E).

Subsequently, the cleaned scallop shells were dried at 100 °C for 1 h using a drying stove QUIMIS Q314M230, San Felipe, Chile (B). The scallop shells were located with their concavity upwards and uniformly inside the stove. Then, the samples were ground in a grinder (C) and sieved with varied sieve sizes (D) to obtain the ranges of sizes particles reported in Table 1 (E).

Table 1. Sieved sample labeling for different particle size ranges of scallop shell waste used.

Sample	Codification	Particle Size Range (μm)
Big size	BS	595–1000
Medium size	MS	250–595
Small size	SS	<250

2.2. Characterization of Scallop Shell Waste

The morphology of the scallop shell powders was determined using a JEOLT T-300, Osaka, Japan scanning electron microscope (SEM) operated at an acceleration voltage of 15–25 kV. The chemical composition of the material was obtained by X-ray fluorescence spectroscopy (XRF) using a Rigaku ZSX Primus II type (WDS), Monterey, CA, USA equipment was used with rhodium radiation without standardization. Specific surface area and pore size distribution of scallop shell waste powders were determined by nitrogen adsorption–desorption isotherms at 77 K using the Brunauer–Emmett–Teller (BET)

analysis and by the Barret–Joyner–Halenda (BJH) method, using a Micromeritics 3Flex version 4.02 adsorption analyzer. The crystallinity and phase of the scallop shells powders were identified by X-ray diffraction (XRD) using a Bruker D4, Massachusetts, USA powder diffractometer equipped with a Lynxse detector and operated with Cu K α radiation, using an angular range between 3 and 70° 2theta with a step of 0.02. The thermal stability and decomposition of scallop shells were determined using differential scanning calorimetry (DSC), Mettler Toledo 822e equipment, Columbus, Ohio, USA. with 40 μ m aluminum capsules using the ASTM D3418 standard. In addition, thermogravimetric analysis (TGA) of the materials was performed with a TA model Q50 using the ISO 11358 standard. The functional and anchoring groups on the surface of the scallop shells powders were identified by Fourier-transform infrared spectroscopy (FTIR) using a thermo Spectrum 65 FTIR spectrometer, Santiago, Chile. mail spectrometer with an MCT detector at a resolution of 1 cm⁻¹ and 32 scan.

2.3. Caffeic Acid Removal Tests

The removal percentage of caffeic acid and arsenic(III) was evaluated using different particle size ranges of scallop shell waste reported in Table 1. To a borosilicate glass batch reactor was added 250 mL of 10 ppm caffeic acid (CA) solution. Subsequently, 500 ppm of scallop shell waste with different diameter ranges of BS, MS, and SS (see Table 1) were added. The suspension was stirred in the dark until 180 min for BS, MS, and SS, respectively.

The reactor's temperature was maintained at room temperature by recirculating tap water through the reactor double jacket while stirring was continuously provided. Samples of 10 mL were taken every 10 min until 180 min were complete. All samples were filtered using a nylon membrane with a pore of 0.22 μ m to remove scallop shell waste.

The removal percentage of caffeic acid was determined using a UV-visible Evolution 220 Thermo Scientific, Mundelein, IL, USA. Absorbance spectra measures were obtained between 200 and 500 nm. In addition, the CA removal percentage was determined using high-resolution liquid chromatography (HPLC) using an Agilent Infinity 1260 chromatograph equipped with a UV-vis diode array detector and a C-18 reverse column. A mixture of acetonitrile:water/formic acid (%) (13:87) was used as a mobile phase, with a flow rate of 0.7 mL min⁻¹ by 12 min. Caffeic acid was determined at a holding time of 8.9 min, setting 324 nm as the wavelength to calculate the pollutant (CA) removal percentage by this technique. Tests with each diameter of scallop shell waste (BS, MS, and SS) were performed three times.

2.4. Arsenic(III) Removal Tests

To remove arsenic(III), the same system used to determine caffeic acid removal was used. Into this system was added 300 mL of a 1.6 ppm arsenic(III) solution. Subsequently, 500 ppm of scallop shell waste with different diameter ranges of BS, MS, and SS (see Table 1) were added. Samples of 30 mL were taken every 10 min until 60 min were complete. All samples were centrifuged for 15 min at 4500 rpm to remove scallop shell waste.

The removal percentage of arsenic(III) was determined using a colorimetric method using a UV-visible Evolution 220 Thermo Scientific. The colorimetric method uses a 30 mL sample aliquoted into a 125 mL frosted Erlenmeyer. After, 70 mL of deionized water was added. A total of 20 mL of concentrated sulfuric acid was added to the same flask and cooled in a water bath to room temperature. At the same time, 0.0100 g of silver diethyldithiocarbamate (DDCT Ag) was weighed in a beaker and dissolved with 5 mL of pyridine; this solution was placed in an arsenic(III) absorption tube, 16 g of granular zinc was added to the frosted Erlenmeyer and connected to the absorption tube, ensuring proper sealing with a clamp (see Figure 2).

The system was left under moderate agitation for two hours. Finally, the absorbance of the solution contained was determined in the range of 450 and 650 nm, setting 523 nm as the wavelength to calculate the arsenic(III) removal percentage by this technique. Tests with each diameter of scallop shell waste (BS, MS and SS) were performed three times.

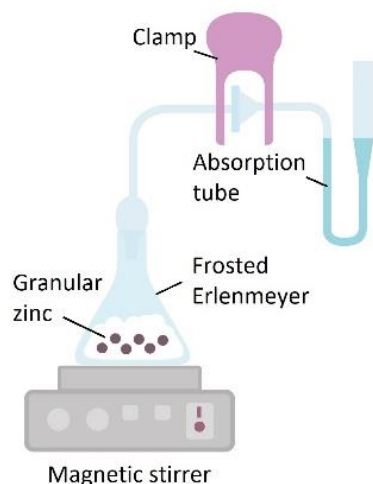


Figure 2. System used for colorimetric determination of arsenic(III).

3. Results

3.1. Characterization of Scallop Shell Waste

Results of the X-ray fluorescence spectroscopy (XRF) analysis show that all samples are mainly composed of calcium in the form of calcium oxide (CaO), which represents more than 97% of the shell composition (Table 2). Therefore, the scallop shell waste are an attractive bio-resource of high-purity calcium carbonate, as shown in various studies of other bivalve shells worldwide [35].

Table 2. Chemical composition of scallop shell waste powder obtained with X-ray fluorescence (XRF).

Oxide	(%)
CaO	97.68
SiO ₂	0.08
Na ₂ O	0.81
Fe ₂ O ₃	0.10
SO ₃	0.35
SrO	0.33
MgO	0.21
Al ₂ O ₃	0.03
P ₂ O ₅	0.40

The crystal structure of the analyzed scallop shell powders (Figure 3) confirms the composition obtained by the XRF technique. These powders have a single phase and correspond to a rhombohedral calcite crystal structure calcite because the diffraction peaks coincide satisfactorily with the JCPDS 05-586 card. The most representative peaks are located at angles (2θ) 23.06°, 29.41°, 31.42°, 35.97°, 39.4°, 43.17°, and 47.48°, corresponding to planes (112), (104), (006), (110), (113), (201), and (018), respectively.

It has to be noted that the scallop shells possess a pure calcite CaCO₃, which differs from most other shells that present an aragonitic phase, and a large part of the species at a global level present both polymorphs, but with an ergonomic predominance [36]. The scallop shell from northern Chile has the same calcite crystalline phase present in commercial CaCO₃ coming from limestone rocks. This scallop shell waste can be used for practically the same industrial applications that use commercial CaCO₃ [37].

In order to determine the thermal behavior of the scallop shell waste powder, it was subjected to differential scanning calorimetry (DSC) with a dynamic variation of temperature at a scanning speed of 10 °C/min. Figure 4 shows that the shell waste powder accumulates heat steadily as the temperature it is subjected to increases. This endothermic behavior can be attributed to the moisture of the organic matter present on the sample.

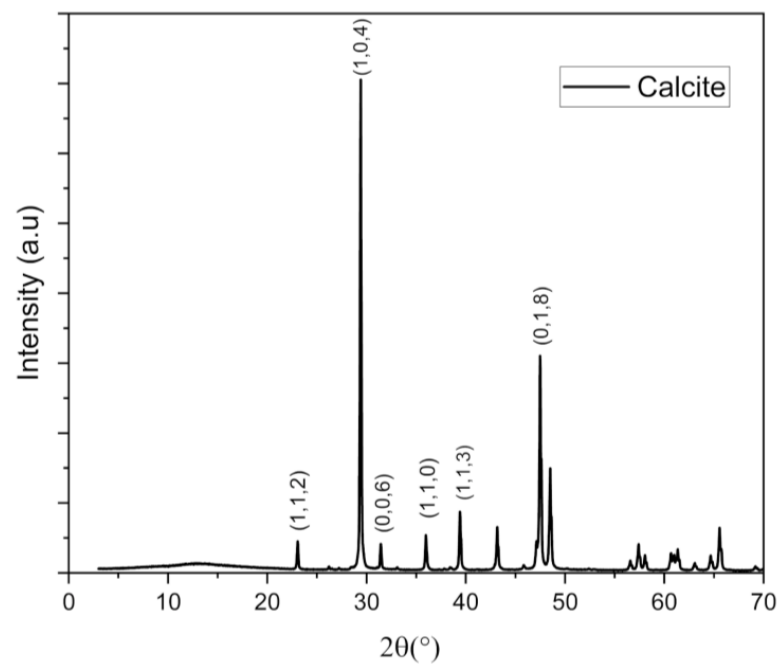


Figure 3. X-ray diffractogram (XRD) of scallop shell waste powder.

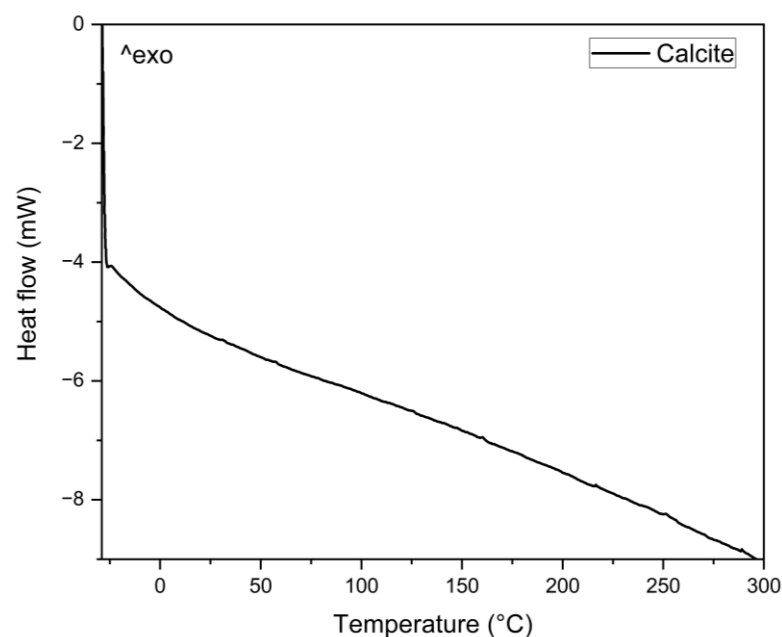


Figure 4. Differential scanning calorimetry (DSC) of scallop shell waste.

Thermogravimetric analysis (TGA) shows the decomposition periods of scallop shell waste powders (Figure 5). In the beginning, the thermogram exhibits a loss of 2.13% in weight coming from the organic matter that seashells have within them, which remains in the crushed samples despite the shells having been washed previously [38].

After 600 °C, a strong reduction in weight can be seen, corresponding to the thermal decomposition of calcium carbonate up to 688.35 °C. Due to the fact that scallop shell waste has very few impurities, it can be assumed that the resulting sample is calcium oxide (CaO), and 42.23% by weight is released as carbon dioxide (CO₂) into the environment, as shown in Equation (1) [39].

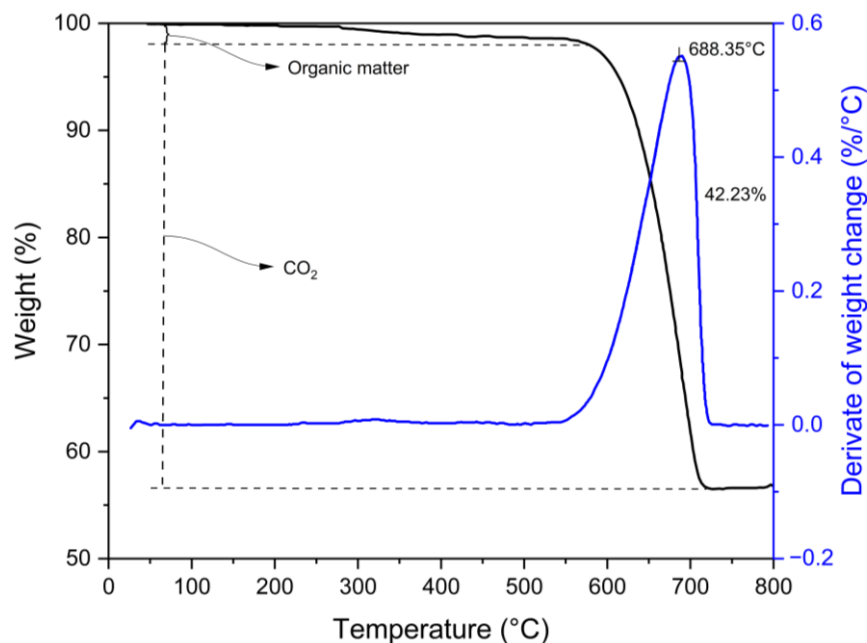


Figure 5. Thermogravimetric analysis (TGA) of scallop shell waste.

Therefore, through this analysis, it is possible to observe the thermal behavior of calcitic CaCO_3 from scallop shells for future applications. Also, a promising bioresource of calcium oxide can be obtained through calcination, a material used for desulfurization, cement manufacturing, as a catalyst to produce biofuels, and as an antimicrobial agent, among others [40–43].



Figure 6 shows the images of scanning electron microscopy (SEM). These images show different magnifications of the scallop shell waste powders obtained for the different ranges of particles studied (BS, MS, and SS). All the powders showed a similar morphology. The morphology of all the scallop shell waste is amorphous. These forms are distributed from fine particles (SS) to more elongated particles (BS), just as smaller particles are found as the amplitude increases used with the microscope.

The morphology presented by scallop shell waste powders is similar to “whiskers”; this name is given to thin structures with a greater length to diameter ratio than what is usually seen. A study shows that by using “whiskers” as reinforcement in the manufacture of composite materials, these “whiskers” improve the mechanical properties of bending, tension, and impact of the obtained polymeric composite materials [44].

SEM images show no differences in the shape of the BS, MS, and SS samples. Nevertheless, there is a decrease in the particle size between the three sizes.

Figure 7 shows the FTIR spectrum of the obtained CaCO_3 SS powder. From the FTIR spectrum profile, it is possible to observe the three characteristics absorption bands of calcite- CaCO_3 , located at 712 cm^{-1} , 870 cm^{-1} , and 1390 cm^{-1} , ascribed to the vibrations of C-O stretching of the CO_3^{2-} [45,46].

The most representative absorption peak at 1390 cm^{-1} is attributed to amorphous calcium carbonate. Also, no bands were observed in the range of $3100\text{ to }3500\text{ cm}^{-1}$, associated with the presence of OH- groups.

Figure 8 shows isotherms of scallop shell waste. The three analyzed materials (BS, MS, and SS) present type IVa isotherms because they show a loop of hysteresis. The hysteresis loop accompanies capillary condensation, which is H3 type; these loops are given by non-rigid aggregates of plate-like particles [47,48]. The SEM images of the analyzed materials confirms the presence of this characteristic. Table 3 reports textural analysis, specifically specific superficies, pore volume, and average pore diameter of the three materials analyzed.

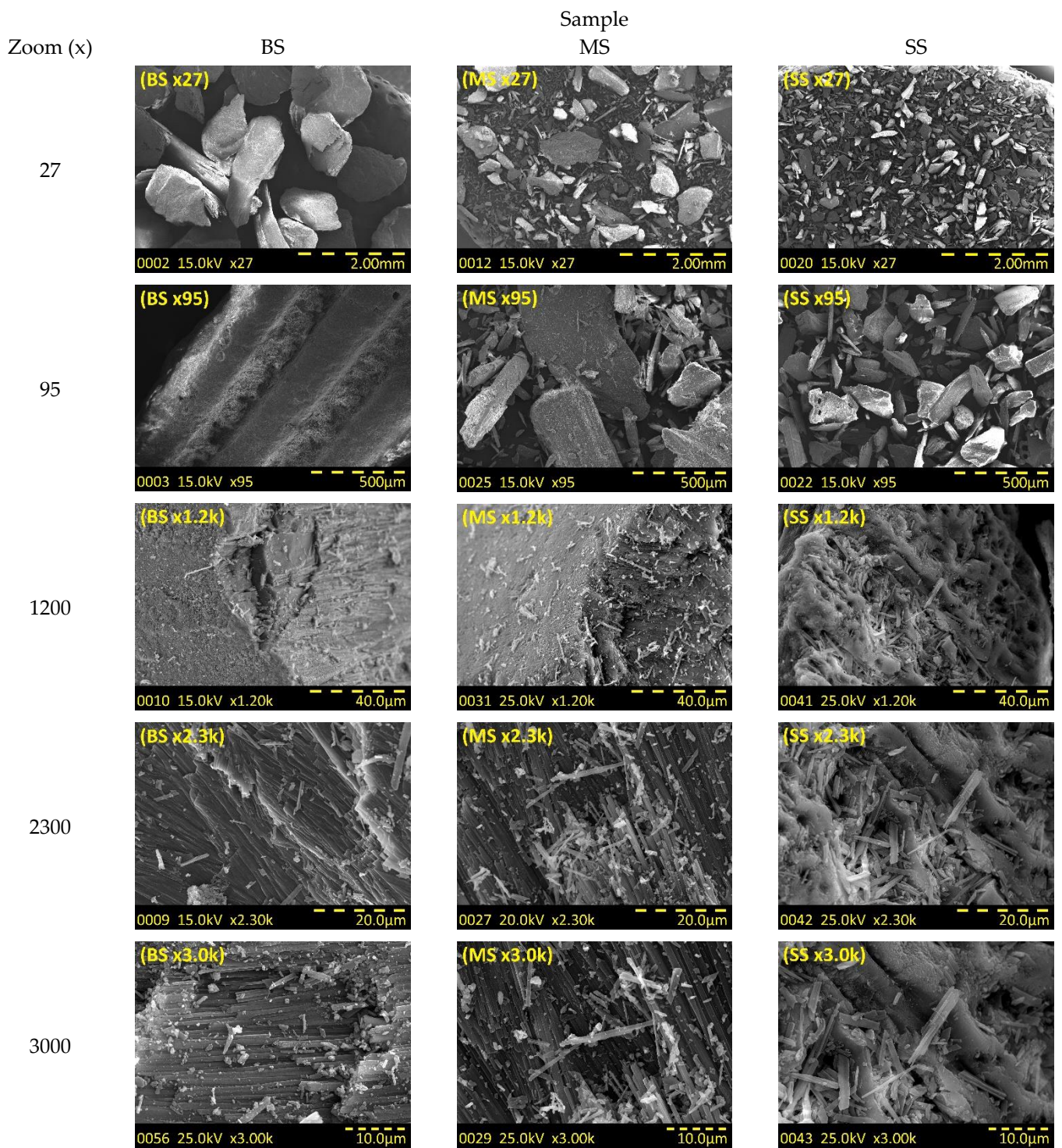


Figure 6. SEM of scallop shells powder. Row 1, 2, 3, 4 and 5: BS, MS, and SS at $\times 27$, $\times 95$, $\times 1.2k$, $\times 2.3k$, and $\times 3.0k$, respectively.

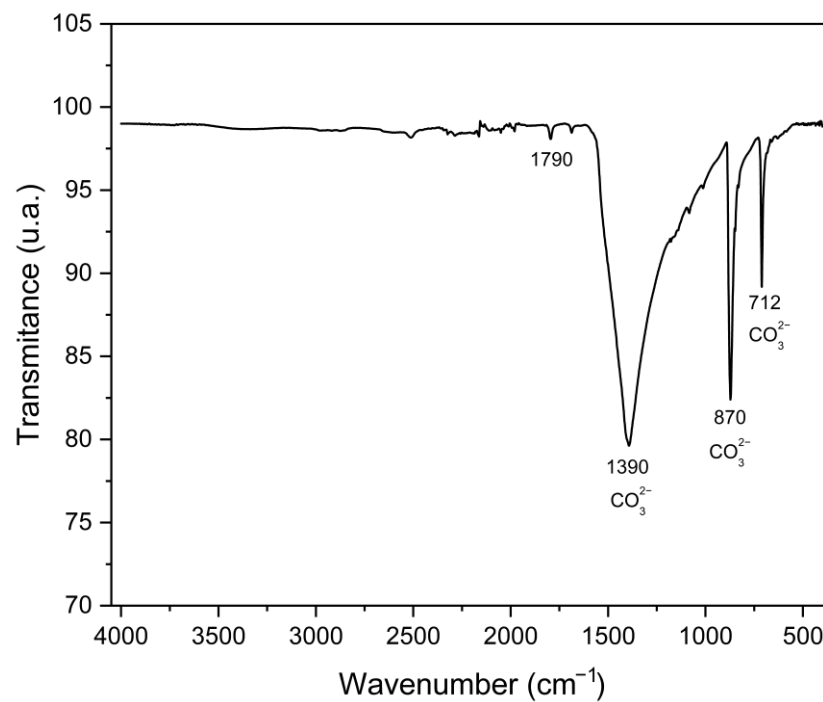


Figure 7. FTIR spectrum of the CaCO₃ SS powder.

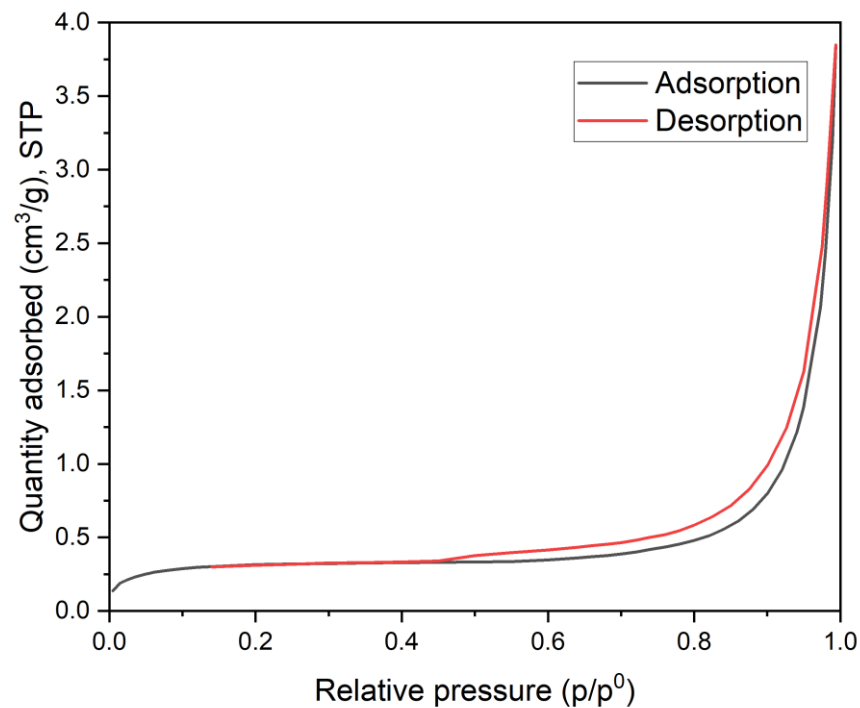


Figure 8. Specific surface area (BET) of scallop shell waste.

Table 3. Textural properties of different particle size ranges and capacity of average contaminants removal percentages for scallop shell waste, $p < 0.0001$.

Sample	Surface Area (m ² /g)	Pore Volume (cm ³ /g)	Average Pore Diameter (nm)	CA Removal Percentage (%)	As(III) Removal Percentage (%)
BS	3	0.0055	7.6	0.0 ± 0.0	10.0 ± 0.6
MS	4	0.0095	10.4	88.0 ± 1.6	17.0 ± 0.2
SS	1	0.0050	18.0	100.0 ± 0.0	23.0 ± 0.3

3.2. Removal of Water Waste Contaminants

Water decontamination tests using scallop shell powder were performed with the objective of defining a potential application for this type of waste. Two of the main contaminants of Chilean waters were selected, the first being Caffeic Acid (CA), which is a compound commonly found in wastewater produced by vitiviniculture [49–53]. The second contaminant selected is Arsenic in the form of As(III), which is present in soil and water bodies [54,55], as well having been found in potable waters [56,57].

Figure 9 shows the removal percentage of caffeic acid (CA) and arsenic(III) obtained using different particle size ranges of scallop shell waste (BS, MS, and SS) for 20 and 80 min, respectively. In Figure 9, scallop shell waste with a small diameter (SS) presents a high removal percentage of contaminants. In addition, the waste with a big particle diameter (BS) presents practically zero removal percentage. This behavior can be explained by textural properties (Table 3). The standard deviation (SD) shows no significant differences between the results obtained, which demonstrates that they are precise and reproducible.

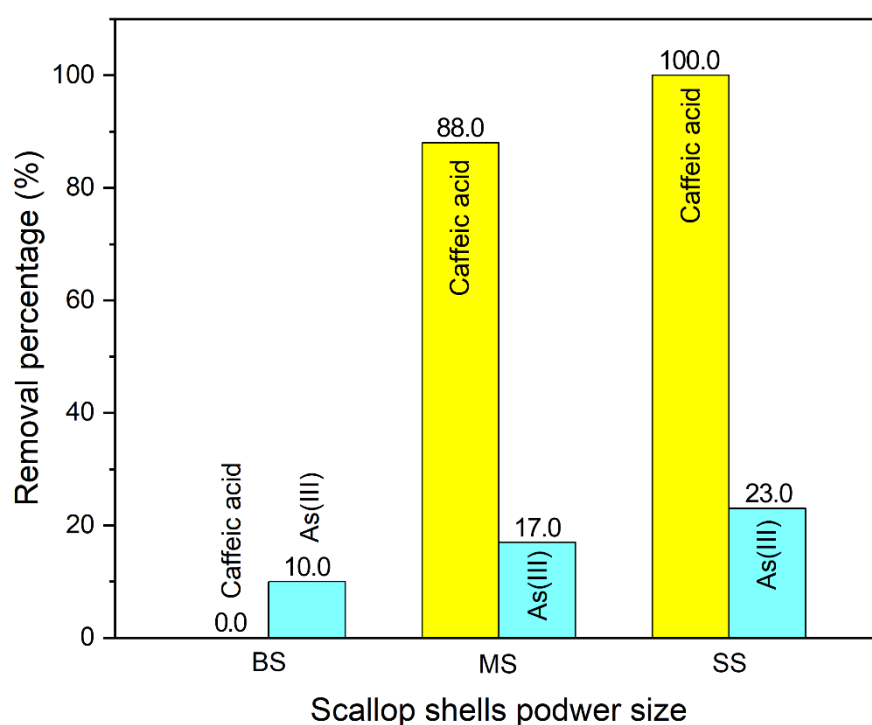


Figure 9. Removal percentage of caffeic acid and arsenic(III) using different particle size ranges of scallop shell residues (BS, MS, and SS).

In order to understand the adsorption process between the scallop shell residues and the caffeic acid contaminant, experiments were carried out by using crushed shell powder with a small particle size (SS) and subjecting them to different operational definitions. This study will, therefore, focus on the effect that variable pH, shell powder concentration, and contaminant concentration have on the adsorption process.

Table 4 shows the removal average percentage of caffeic acid by different SS-sized shell powder concentrations. The SD shows no significant differences between the results obtained, and the results indicate that, while adsorption percentages do not deviate significantly between samples after 90 min, they do vary after 20 min, with the 1000 ppm sample having the highest adsorption percentage amongst samples. This behavior clearly suggests that increasing the concentration of northern scallop shell residue would hasten the removal of caffeic acid from the system in this study.

Table 4. Adsorption percentage and pH variation after 90 min using different northern scallop shell concentrations, $p < 0.0001$.

Sample Concentration (ppm)	Adsorption (%) 20 min	Adsorption (%) 90 min	Starting pH	Final pH
200	54.2 ± 0.4	85.4 ± 0.3	4.6	7.0
500	74.4 ± 0.5	98.5 ± 0.2	4.5	6.8
1000	84.2 ± 0.4	98.6 ± 0.2	4.6	9.1

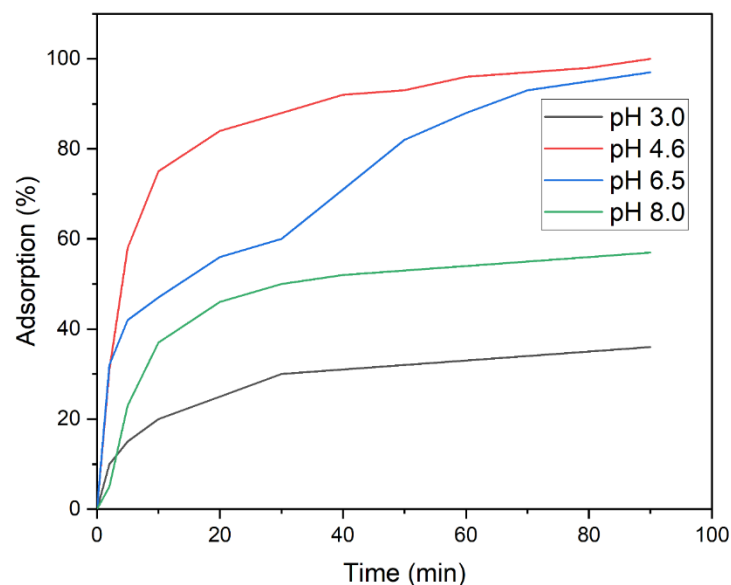
It is also important to note that caffeic acid adsorption reaches its maximum value after 80 min, as results from the 500 ppm and 1000 ppm samples are almost identical, with 98.5% and 98.6%, respectively, and remain constant until the end of the experiment at 90 min, implying that the majority of caffeic acid has already been adsorbed by the shell residue. This, in turn, means that increasing shell residue concentration above 500 ppm becomes unnecessary for this system.

Furthermore, increasing residue concentration to 1000 ppm has an effect on final sample pH, increasing it well above the limit allowed by international law regarding water reuse. Final pH values of the other two samples are both within the 6.5 to 8.0 range required by law.

The post-adsorption pH increase is caused by the calcium carbonate that makes up the scallop shells, as it is an oxysalt that increases pH in contact with water, therefore increasing system pH as the shell residue concentration increases.

Results are presented as mean ± standard deviation. We compared CA removal percentage and As(III) removal percentage among the three surface area groups (BS, MS, SS) by means of an unifactorial ANOVA model (Table 3). We did likewise for adsorption (Table 4), comparing three levels of sample concentration. Removal percentage of caffeic acid at different initial pH values was compared by a multiple linear regression model, considering time in logarithmic scale.

Initial sample pH and its effects on adsorption rates were also studied. Removal percentages remain low at pH 3.0 ($34.1 \pm 0.6\%$) and pH 8.0 ($57.7 \pm 0.6\%$), while pH values for 4.6 and 6.5 yielded adsorption percentages of $100.0 \pm 0.0\%$ and $97.3 \pm 0.4\%$, respectively. It is important to note that the adsorption process slows down at pH 6.5, meaning that this pH value would be most useful in a situation where contaminants need to be removed in a controlled manner, as shown in Figure 10.

**Figure 10.** Removal percentage of caffeic acid at different initial pH values; pH and time effect are statistically significant ($p < 0.0001$).

The initial pH value selected for this study was of 4.6, as it allows for a faster caffeic acid adsorption rate while also needing no previous adjustments to sample pH.

The adsorption behaviors seen in Figure 10 can be explained by calcium carbonate's point of zero charge value of 8.3 [58]. Below this point, the carbonate compound's surface charge remains positive, while at pH values above 8.3, surface charge becomes negative. Furthermore, a pH 3.0 caffeic acid solution has a neutral charge, which makes its adsorption onto the shell residue difficult. Increasing pH to 5.0 negatively polarizes caffeic acid by about 70%, and further increasing pH to 7.0, caffeic acid polarization increases to about 100%, making it easier for it to be adsorbed onto the shell residue's surface.

On the other hand, at a pH value of 8.0, calcium carbonate's surface charge is almost neutral; therefore, the seashell residue's capacity to adsorb contaminants begins to decrease, as the primary intermolecular forces acting at this point are Van der Waals forces.

In addition, high adsorption percentages were observed at pH values of 4.6 and 6.5. This can be explained by the seashell residue's surface being positively charged while the caffeic acid contaminant is negatively charged at this pH range, as shown in Figure 11, enabling the adsorption process through an electrostatic interaction between shell residue and contaminant.

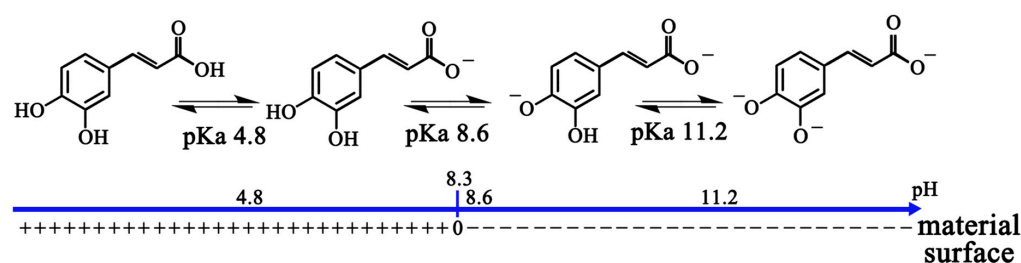


Figure 11. Surface charge of calcium carbonate and caffeic acid at different pH values.

Table 5 shows the variation in contaminant concentration during the adsorption tests over a timespan of 90 min. The removal percentage of a starting caffeic acid concentration of 10 ppm is 69.2%, while doubling that initial concentration to 20 ppm yields a removal percentage of 34.9%, an efficiency reduction of almost 50%, which suggests that a 500 ppm sample of shell residue may only remove up to 10 ppm of caffeic acid at a time, leaving the rest in solution due to the saturation of the material's surface.

Table 5. Effect of contaminant concentration on adsorption percentage and pH variation.

Caffeic Acid Concentration (ppm)	Adsorption (%)	Starting pH	Final pH
10	69.2 ± 0.4	4.4	6.8
20	34.9 ± 0.3	4.4	8.7

The final pH values in Table 5 show that increasing the caffeic acid contaminant's concentration also increases pH. All conditions analyzed in this work determine that 500 ppm of shell residue are needed in order to remove 10 ppm of caffeic acid out of a water sample, as well as a pH value of 4.6 and a timespan of 90 min, allowing for high adsorption percentages of the contaminant on the seashell powder.

Conversely, arsenic removal testing did not include setting new operational definitions, as the studies on this subject were directly carried out on water meant for human consumption, and thus working conditions were defined by their characteristics. The adsorption mechanism for this system consists of arsenic ions gathering on the shell residue's surface. Initially, these ions interact with the material's surface through electrostatic forces, subsequently diffusing through its pores until finally settling down on the capillary spaces of the material used as an adsorbent [59–61].

Table 6 shows a comparison between the removal percentages obtained in this work and those of materials commonly used in wastewater treatment for these specific contaminants. Results indicate that northern scallop shell waste has a high potential in water

decontamination applications, as many of the adsorbents reported on Table 6 are either synthesized by using several chemical reagents [62–66], have a high energy consumption [67–71], or require large infrastructures [69–72] compared to scallop shell waste, which is processed at a low energy cost and does not require complex infrastructure nor any additional chemical reagent.

Table 6. Comparison of capacity of contaminants removal percentages of Chilean scallop shell waste with other adsorbents.

Adsorbent	pH	CA Removal Percentage (%)	As(III) Removal Percentage (%)	Reference
BS	4.3	0	10.0	This work
MS	4.3	88.0	17.0	This work
SS	4.3	100.0	23.0	This work
Chitosan	5.0	12.0	-	[73]
Magnetic Activated Carbon	3.0	97.0	-	[74]
Polystyrene Crosslinked with Divinylbenzene	-	91.0	-	[75]
TiO ₂ -Mt-Ce-Mn	7.0–8.0	-	97.88	[64]
Fe ₃ O ₄ @Cu/Ce	5.0	-	75.0	[68]
Chitosan	8.5	-	71.7	[70]
Chitosan	5.0–10.0	-	>95.0	[72]

Figure 12 shows the pore size distribution of the different particle size ranges of scallop shell waste (BS, MS, and SS) used in this study, which was determined by the Barret–Joyner–Halenda (BJH) method. It can be seen that the removal percentage of caffeic acid (CA) and arsenic(III) is higher in the material with a lower surface area (SS). However, the pore size distribution (nm) plays an important role as BS and MS materials have larger specific surfaces, but according to pore size distribution, the pores in these materials present sizes between 3 and 12 nm, much smaller than the SS material (7.5 and 30 nm). The BS and MS samples exhibited a much more limited pore size distribution, presenting pores only up to 20 nm.

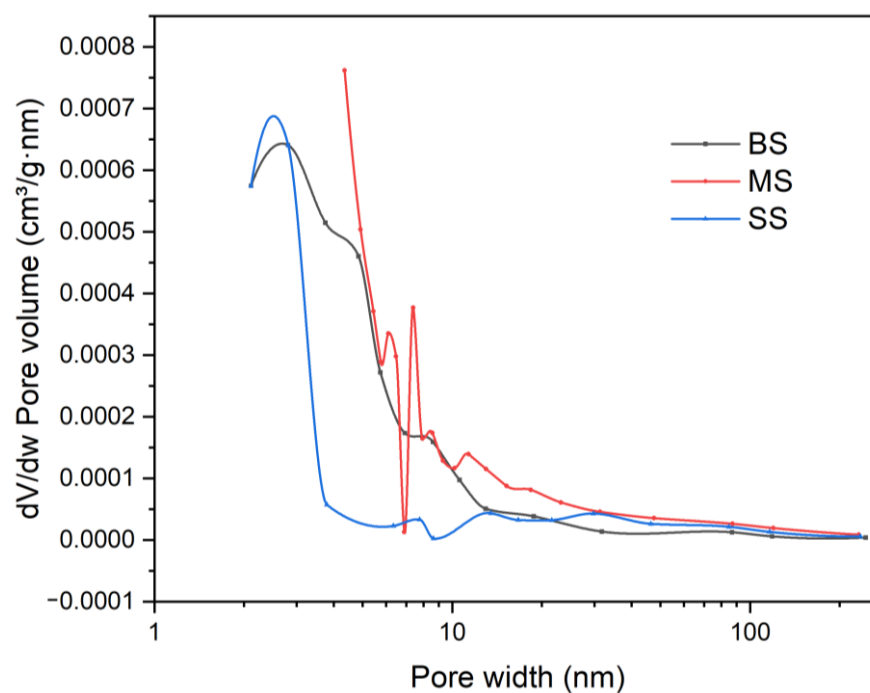


Figure 12. Pore size distribution using different particle size ranges of scallop shells residues (BS, MS, and SS).

The present study shows a direct correlation between the textural properties of scallop shell waste, especially with pore size distribution, and the removal of contaminants in the water. A larger pore size favors a high removal percentage of target contaminants caffeic acid and arsenic(III) from water, regardless of the specific surface area of the material. Properties such as morphology, chemical composition, and functional groups do not strongly affect the removal of pollutants using this waste as material for water treatment.

3.3. Potential Use of Scallop Shells Residues for Composite Materials

Results obtained over the course of this work regarding the characterization of northern Chile scallop shell powders show that this waste has a low processing cost as well as high purity. Moreover, it is a promising material for the development of composite materials, as the morphology of these powders is similar to those used for coating protections [76] and for the development of a novel geopolymeric matrix composite reinforced with basalt fiber [77]. Alam and Chowdhury [78] obtained a novel material composed of an epoxy matrix reinforced with $\text{CaCO}_3\text{-Al}_2\text{O}_3\text{-MgO-TiO}_2/\text{CuO}$, wherein they demonstrated that an increase in CaCO_3 improved certain physical properties of the material, namely tensile and flexural strength, as well as impact resistance. DSC and TGA curves for the CaCO_3 used in their work are very similar to those obtained for northern Chile scallop shells. The DSC curves by Fombuena et al. [34] shows that shell waste powder does not precipitate when used as reinforcement in the manufacture of epoxy resin matrix composite materials.

Kota et al. [79] increased CaCO_3 by 5%, obtaining a hardness increase of 3.14% and a 40% increase to the elastic modulus of a hybrid composite material composed of a polymeric matrix reinforced with glass fiber and polyphenylene sulfide. Echeverria et al. [80] improved the mechanic properties of a bio-composite material containing bivalve mollusk seashell (Verenidae) extracted from the shores of Australia, and the CaCO_3 they used had a pore size comparable to that in the present work. Wang et al. [81] obtained a 22% increase in tensile stress and a 17% increase in bending strength on a starch/fiber foaming composite material using a similar particle size to the ones in this work, as well as FTIR peaks of 875 cm^{-1} .

4. Conclusions

For the first time, this study uses different techniques to determine the properties of scallop shell waste from northern Chile. This characterization allows us to define potential applications for this waste, especially in the manufacture of composite materials to promote a circular economy.

These wastes can also be used as material for water treatment due to their morphology, chemical composition, thermal stability, and surface functional groups. It was determined that the SS granulometry ($<250\text{ }\mu\text{m}$) of the scallop shell waste shows the best removal percentages of caffeic acid (100.0%) and arsenic III (23.0%) from water.

Tests developed using SS granulometry showed that the best conditions for favorable removal of the phenolic compound from water were using a pH close to 4.6 and a concentration of 500 ppm of scallop shell waste from northern Chile.

Properties such as morphology and chemical composition do not significantly affect the removal of target contaminants using scallop shell waste as a decontaminating material. Therefore, high removal percentages of such compounds can be largely attributed to the pore size distribution of the shell powder, being a key property for this process regardless of specific surface areas in each material.

To sum up, the results show that it is viable to use scallop shell waste generated in northern Chile to remove contaminants present in wastewater of the wine industry (caffeic acid) and drinking water (arsenic III).

Author Contributions: Conceptualization, P.Z.S. and A.A.-A.; methodology, A.A.-A. and A.C.M.; software, M.V.F. and A.D.C.; validation, A.C.M., J.L.V.R. and A.A.-A.; formal analysis, A.C.M.; C.A.N.R. and A.A.-A.; investigation, P.Z.S.; writing—original draft preparation, P.Z.S. and M.V.F.; writing—review and editing, A.C.M. and A.A.-A.; supervision, A.C.M. and A.A.-A.; project administration,

A.A.-A.; funding acquisition, A.C.M. and A.A.-A. All authors have read and agreed to the published version of the manuscript.

Funding: The authors would like to thank the financial support of DIDULS/ULS, through the projects PR21172 and PR2153857. Acknowledges the financial support of DIDULS/ULS through the project FIULS 2030 grant number 18ENI2-104235 funded by the CORFO program “Nueva Ingeniería para el 2030 en Regiones—Etapa de Implementación”, Multidisciplinary R&D Project DIDULS FIULS 2030 N_ID1953851, FONDEQUIP EQM-160070 and FONDEQUIP 150109.

Institutional Review Board Statement: Not applicable.

Informed Consent Statement: Not applicable.

Data Availability Statement: The data presented in this study are available on request from the corresponding author. The data are not publicly available due to publicly.

Conflicts of Interest: The authors declare no conflict of interest.

References

1. FAO. *The State of World Fisheries and Aquaculture 2020*; FAO: Rome, Italy, 2020.
2. Tokeshi, M.; Ota, N.; Kawai, T. A comparative study of morphometry in shell-bearing molluscs. *J. Zool.* **2000**, *251*, 31–38. [CrossRef]
3. Kapranov, S.V.; Karavantseva, N.V.; Bobko, N.I.; Ryabushko, V.I.; Kapranova, L.L. Element Contents in Three Commercially Important Edible Mollusks Harvested off the Southwestern Coast of Crimea (Black Sea) and Assessment of Human Health Risks from Their Consumption. *Foods* **2021**, *10*, 2313. [CrossRef]
4. Khasreen, M.M.; Banfill, P.F.G.; Menzies, G.F. Life-Cycle Assessment and the Environmental Impact of Buildings: A Review. *Sustainability* **2009**, *1*, 674–701. [CrossRef]
5. Kobatake, H.; Kirihara, S. Lowering the incineration temperature of fishery waste to optimize the thermal decomposition of shells and spines. *Fish. Sci.* **2019**, *85*, 573–579. [CrossRef]
6. Summa, D.; Lanzoni, M.; Castaldelli, G.; Fano, E.A.; Tamburini, E. Trends and Opportunities of Bivalve Shells’ Waste Valorization in a Prospect of Circular Blue Bioeconomy. *Resources* **2022**, *11*, 48. [CrossRef]
7. Topić Popović, N.; Lorencin, V.; Strunjak-Perović, I.; Čož-Rakovac, R. Shell Waste Management and Utilization: Mitigating Organic Pollution and Enhancing Sustainability. *Appl. Sci.* **2023**, *13*, 623. [CrossRef]
8. Vásquez, R.M.C. Manual de Buenas Prácticas Para el Cultivo de Moluscos Bivalvos. OIRSAOSPESCA. 2014, p. 117. Available online: https://isamx.org/sitio/pdfs/Manual%20de_BPde_M_Version%20Digital_011014155613.pdf (accessed on 16 April 2024).
9. Avendaño, R.E.; Riquelme, C.E.; Escribano, R.; Reyes, N. Postlarval survival and growth of *Argopecten purpuratus* (Lamarck, 1819) in Bahía Inglesa, Chile: Effects of origin, distribution in the bay and larval bacterioflora. *Rev. Chil. Hist. Nat.* **2001**, *74*, 669–679. [CrossRef]
10. Bakit, J.; Álvarez, G.; Díaz, P.A.; Uribe, E.; Sfeir, R.; Villasante, S.; Bas, T.G.; Lira, G.; Pérez, H.; Hurtado, A.; et al. Disentangling Environmental, Economic, and Technological Factors Driving Scallop (*Argopecten purpuratus*) Aquaculture in Chile. *Fishes* **2022**, *7*, 380. [CrossRef]
11. Anuarios Estadísticos de Pesca y Acuicultura | Servicio Nacional de Pesca y Acuicultura. (s. f.). Available online: <https://www.sernapesca.cl/informacion-utilidad/anuarios-estadisticos-de-pesca-y-acuicultura/> (accessed on 5 April 2024).
12. Valenzuela, B.A.; Yáñez, C.G.; Golusda, V.C. El Ostión del Norte Chileno (*Argopecten Purpuratus*), un Alimento de Alto Valor Nutricional. *Rev. Chil. Nutr.* **2011**, *38*, 148–155. [CrossRef]
13. Silva, T.; Mesquita-Guimarães, J.; Henriques, B.; Silva, F.S.; Fredel, M.C. The Potential Use of Oyster Shell Waste in New Value-Added By-Product. *Resources* **2019**, *8*, 13. [CrossRef]
14. Nash, K.L.; Blythe, J.L.; Cvitanovic, C.; Fulton, E.A.; Halpern, B.S.; Milner-Gulland, E.J.; Addison, P.F.E.; Pecl, G.T.; Watson, R.A.; Blanchard, J.L. To Achieve a Sustainable Blue Future, Progress Assessments Must Include Interdependencies between the Sustainable Development Goals. *One Earth* **2020**, *2*, 161–173. [CrossRef]
15. Marin, F.; Luquet, G. Molluscan shell proteins. *Comptes Rendus Palevol* **2004**, *3*, 469–492. [CrossRef]
16. Bar-Yosef Mayer, D.E. Shell ornaments and artifacts in Neolithic Cyprus and correlations with other Mediterranean regions. *Quat. Int.* **2018**, *464*, 206–215. [CrossRef]
17. Gamble, L.H. The origin and use of shell bead money in California. *J. Anthropol. Archaeol.* **2020**, *60*, 101237. [CrossRef]
18. Yoon, H.; Park, S.; Lee, K.; Park, J. Oyster shell as substitute for aggregate in mortar. *Waste Manag. Res.* **2004**, *22*, 158–170. [CrossRef]
19. Yang, E.-I.; Kim, M.-Y.; Park, H.-G.; Yi, S.-T. Effect of partial replacement of sand with dry oyster shell on the long-term performance of concrete. *Constr. Build. Mater.* **2010**, *24*, 758–765. [CrossRef]
20. Ohimain, E.I.; Basse, S.; Bawo, D.D.S. Uses of sea shells for civil construction works in coastal Bayelsa State, Nigeria: A waste management perspective. *Res. J. Biol. Sci.* **2009**, *4*, 1025–1031.

21. Barros, M.C.; Bello, P.M.; Bao, M.; Torrado, J.J. From waste to commodity: Transforming shells into high purity calcium carbonate. *J. Clean. Prod.* **2009**, *17*, 400–407. [[CrossRef](#)]
22. Lee, C.H.; Lee, D.K.; Ali, M.A.; Kim, P.J. Effects of oyster shell on soil chemical and biological properties and cabbage productivity as a liming materials. *Waste Manag.* **2008**, *28*, 2702–2708. [[CrossRef](#)]
23. Xing, R.; Qin, Y.; Guan, X.; Liu, S.; Yu, H.; Li, P. Comparison of antifungal activities of scallop shell, oyster shell and their pyrolyzed products. *Egypt. J. Aquat. Res.* **2013**, *39*, 83–90. [[CrossRef](#)]
24. Yang, X.; Huang, Y.; Liu, K.; Zheng, C. Effects of oyster shell powder on leaching characteristics of nutrients in low-fertility latosol in South China. *Environ. Sci. Pollut. Res.* **2022**, *29*, 56200–56214. [[CrossRef](#)] [[PubMed](#)]
25. Wu, B.; Li, J.; Sheng, M.; Peng, H.; Peng, D.; Xu, H. The application of biochar and oyster shell reduced cadmium uptake by crops and modified soil fertility and enzyme activities in contaminated soil. *SOIL* **2022**, *8*, 409–419. [[CrossRef](#)]
26. Hong, C.O.; Kim, S.Y.; Gutierrez, J.; Owens, V.N.; Kim, P.J. Comparison of oyster shell and calcium hydroxide as liming materials for immobilizing cadmium in upland soil. *Biol. Fertil. Soils* **2010**, *46*, 491–498. [[CrossRef](#)]
27. Ok, Y.S.; Oh, S.E.; Ahmad, M.; Hyun, S.; Kim, K.R.; Moon, D.H.; Lee, S.S.; Lim, K.J.; Jeon, W.T.; Yang, J.E. Effects of natural and calcined oyster shells on Cd and Pb immobilization in contaminated soils. *Environ. Earth Sci.* **2010**, *61*, 1301–1308. [[CrossRef](#)]
28. Moon, D.H.; Koutsospyros, A. Stabilization of Lead-Contaminated Mine Soil Using Natural Waste Materials. *Agriculture* **2022**, *12*, 367. [[CrossRef](#)]
29. Kwon, H.-B.; Lee, C.-W.; Jun, B.-S.; Yun, J.; Weon, S.-Y.; Koopman, B. Recycling waste oyster shells for eutrophication control. *Resour. Conserv. Recycl.* **2004**, *41*, 75–82. [[CrossRef](#)]
30. Liu, Y.-X.; Yang, T.O.; Yuan, D.-X.; Wu, X.-Y. Study of municipal wastewater treatment with oyster shell as biological aerated filter medium. *Desalination* **2010**, *254*, 149–153. [[CrossRef](#)]
31. Jung, S.; Heo, N.S.; Kim, E.J.; Oh, S.Y.; Lee, H.U.; Kim, I.T.; Hur, J.; Lee, G.W.; Lee, Y.C.; Huh, Y.S. Feasibility test of waste oyster shell powder for water treatment. *Process Saf. Environ. Prot.* **2016**, *102*, 129–139. [[CrossRef](#)]
32. Hsu, T.-C. Experimental assessment of adsorption of Cu^{2+} and Ni^{2+} from aqueous solution by oyster shell powder. *J. Hazard. Mater.* **2009**, *171*, 995–1000. [[CrossRef](#)]
33. Rahman, M.A.; Rahman, M.A.; Samad, A.; Shafiqul Alam, A.M. Removal of Arsenic with Oyster shell: Experimental Measurements. *Pak. J. Anal. Environ. Chem.* **2008**, *9*, 2.
34. Fombuena, V.; Bernardi, L.; Fenollar, O.; Boronat, T.; Balart, R. Characterization of green composites from biobased epoxy matrices and bio-fillers derived from seashell wastes. *Mater. Des.* **2014**, *57*, 168–174. [[CrossRef](#)]
35. Moustafa, H.; Youssef, A.M.; Duquesne, S.; Darwish, N.A. Characterization of bio-filler derived from seashell wastes and its effect on the mechanical, thermal, and flame retardant properties of ABS composites. *Polym. Compos.* **2017**, *38*, 2788–2797. [[CrossRef](#)]
36. Lu, J.; Lu, Z.; Li, X.; Xu, H.; Li, X. Recycling of shell wastes into nanosized calcium carbonate powders with different phase compositions. *J. Clean. Prod.* **2015**, *92*, 223–229. [[CrossRef](#)]
37. Islam, K.N.; Bakar, M.Z.B.A.; Noordin, M.M.; Hussein, M.Z.B.; Rahman, N.S.B.A.; Ali, M.E. Characterisation of calcium carbonate and its polymorphs from cockle shells (*Anadara granosa*). *Powder Technol.* **2011**, *213*, 188–191. [[CrossRef](#)]
38. Sophia, M.; Sakthieswaran, N. Waste shell powders as valuable bio- filler in gypsum plaster—Efficient waste management technique by effective utilization. *J. Clean. Prod.* **2019**, *220*, 74–86. [[CrossRef](#)]
39. Mohamed, M.; Yusup, S.; Maitra, S. Decomposition Study of Calcium Carbonate in Cockle Shell. *J. Eng. Sci. Technol.* **2012**, *7*, 1.
40. Rezakazemi, M.; Zhang, Z. 2.29 Desulfurization Materials. In *Comprehensive Energy Systems*; Dincer, I., Ed.; Elsevier: Oxford, 2018; pp. 944–979. ISBN 978-0-12-814925-6.
41. Wagh, A.S. Chapter 13—Calcium Phosphate Cements. In *Chemically Bonded Phosphate Ceramics*, 2nd ed.; Wagh, A.S., Ed.; Elsevier: Amsterdam, The Netherlands, 2016; pp. 165–178. ISBN 978-0-08-100380-0.
42. Lam, M.K.; Lee, K.T. Chapter 15—Production of Biodiesel Using Palm Oil. In *Biofuels*; Pandey, A., Larroche, C., Ricke, S.C., Dussap, C.-G., Gnansounou, E., Eds.; Academic Press: Amsterdam, The Netherlands, 2011; pp. 353–374. ISBN 978-0-12-385099-7.
43. Lahiri, D.; Nag, M.; Ghosh, S.; Ray, R.R. Chapter 8—Green synthesis of nanoparticles and their applications in the area of bioenergy and biofuel production. In *Nanomaterials*; Kumar, R.P., Bharathiraja, B., Eds.; Academic Press: Cambridge, MA, USA, 2021; pp. 195–219. ISBN 978-0-12-822401-4.
44. Jing, Y.; Nai, X.; Dang, L.; Zhu, D.; Wang, Y.; Dong, Y.; Li, W. Reinforcing polypropylene with calcium carbonate of different morphologies and polymorphs. *Sci. Eng. Compos. Mater.* **2018**, *25*, 745–751. [[CrossRef](#)]
45. Dos Santos, V.H.J.M.; Pontin, D.; Ponzi, G.G.D.; Stepanha, A.S.D.G.; Martel, R.B.; Schütz, M.K.; Einloft, S.M.O.; Dalla Vecchia, F. Application of Fourier Transform infrared spectroscopy (FTIR) coupled with multivariate regression for calcium carbonate (CaCO_3) quantification in cement. *Constr. Build. Mater.* **2021**, *313*, 125413. [[CrossRef](#)]
46. Kim, B.-J.; Park, E.-H.; Choi, K.; Kang, K.-S. Synthesis of CaCO_3 using CO_2 at room temperature and ambient pressure. *Mater. Lett.* **2017**, *190*, 45–47. [[CrossRef](#)]
47. Nie, B.; Liu, X.; Yang, L.; Meng, J.; Li, X. Pore structure characterization of different rank coals using gas adsorption and scanning electron microscopy. *Fuel* **2015**, *158*, 908–917. [[CrossRef](#)]
48. Milosevic, M.; Berets, S.L. A Review of Ft-Ir Diffuse Reflection Sampling Considerations. *Appl. Spectrosc. Rev.* **2002**, *37*, 347–364. [[CrossRef](#)]
49. Donoso-Bravo, A.; Rosenkranz, F.; Valdivia, V.; Torrijos, M.; Ruiz-Filippi, G.; Chamy, R. Anaerobic sequencing batch reactor as an alternative for the biological treatment of wine distillery effluents. *Water Sci. Technol.* **2009**, *60*, 1155–1160. [[CrossRef](#)] [[PubMed](#)]

50. Tri, N.L.M.; Thang, P.Q.; Van Tan, L.; Huong, P.T.; Kim, J.; Viet, N.M.; Phuong, N.M.; Al Tahtamouni, T.M. Removal of phenolic compounds from wastewaters by using synthesized Fe-nano zeolite. *J. Water Process Eng.* **2020**, *33*, 101070. [[CrossRef](#)]
51. Genethliou, C.; Kornaros, M.; Dailianis, S. Biodegradation of olive mill wastewater phenolic compounds in a thermophilic anaerobic upflow packed bed reactor and assessment of their toxicity in digester effluents. *J. Environ. Manag.* **2020**, *255*, 109882. [[CrossRef](#)] [[PubMed](#)]
52. Shepherd, H.L.; Grismer, M.E.; Tchobanoglous, G. Treatment of High-Strength Winery Wastewater Using a Subsurface-Flow Constructed Wetland. *Water Environ. Res.* **2001**, *73*, 394–403. [[CrossRef](#)]
53. Melamane, X.L.; Strong, P.J.; Burgess, J.E. Treatment of Wine Distillery Wastewater: A Review with Emphasis on Anaerobic Membrane Reactors. *South Afr. J. Enol. Vitic.* **2007**, *28*, 25–36. [[CrossRef](#)]
54. Osuna-Martínez, C.C.; Armienta, M.A.; Bergés-Tiznado, M.E.; Páez-Osuna, F. Arsenic in waters, soils, sediments, and biota from Mexico: An environmental review. *Sci. Total Environ.* **2021**, *752*, 142062. [[CrossRef](#)] [[PubMed](#)]
55. Zohra, F.T.; Afsin, A.; Al Mamun, A.; Rahaman, M.A.; Rahman, M.M. Source and Distribution of Arsenic in Soil and Water Ecosystem. In *Arsenic Toxicity Remediation: Sustainable Nexus Approach*; Kumar, N., Hashmi, M.Z., Wang, S., Eds.; Springer Nature Switzerland: Cham, Switzerland, 2024; pp. 27–46. ISBN 978-3-031-52614-5.
56. Becar, H.C.; Venegas, G. Impacto y consecuencias del Arsénico en la salud y el medio ambiente en el Norte de Chile. *Rev. Interam. Ambiente Tur. -RIAT* **2012**, *6*, 53–60.
57. Daniele, L.; Cannatelli, C.; Buscher, J.T.; Bonatici, G. Chemical composition of Chilean bottled waters: Anomalous values and possible effects on human health. *Sci. Total Environ.* **2019**, *689*, 526–533. [[CrossRef](#)] [[PubMed](#)]
58. Somasundaran, P.; Agar, G.E. The zero point of charge of calcite. *J. Colloid Interface Sci.* **1967**, *24*, 433–440. [[CrossRef](#)]
59. Garelick, H.; Jones, H.; Dybowska, A.; Valsami-Jones, E. Arsenic Pollution Sources. In *Reviews of Environmental Contamination Volume 197: International Perspectives on Arsenic Pollution and Remediation*; Springer: New York, NY, USA, 2008; pp. 17–60. ISBN 978-0-387-79284-2.
60. Yin, C.Y.; Aroua, M.K.; Daud, W.M.A.W. Review of modifications of activated carbon for enhancing contaminant uptakes from aqueous solutions. *Sep. Purif. Technol.* **2007**, *52*, 403–415. [[CrossRef](#)]
61. Maiti, A.; Mishra, S.; Chaudhary, M. Chapter 25—Nanoscale Materials for Arsenic Removal From Water. In *Nanoscale Materials in Water Purification*; Micro and Nano Technologies; Thomas, S., Pasquini, D., Leu, S.-Y., Gopakumar, D.A., Eds.; Elsevier: Amsterdam, The Netherlands, 2019; pp. 707–733. ISBN 978-0-12-813926-4.
62. Li, H.; Nie, L.; Yao, S. Adsorption Isotherms and Sites Distribution of Caffeic Acid—Imprinted Polymer Monolith from Frontal Analysis. *Chromatographia* **2004**, *60*, 425–431. [[CrossRef](#)]
63. Du, N.; Cao, S.; Yu, Y. Research on the adsorption property of supported ionic liquids for ferulic acid, caffeic acid and salicylic acid. *J. Chromatogr. B* **2011**, *879*, 1697–1703. [[CrossRef](#)] [[PubMed](#)]
64. Lin, Z.; Puls, R.W. Adsorption, desorption and oxidation of arsenic affected by clay minerals and aging process. *Environ. Geol.* **2000**, *39*, 753–759. [[CrossRef](#)]
65. Mudzielwana, R.; Gitari, M.W.; Ndungu, P. Uptake of As(V) from Groundwater Using Fe-Mn Oxides Modified Kaolin Clay: Physicochemical Characterization and Adsorption Data Modeling. *Water* **2019**, *11*, 1245. [[CrossRef](#)]
66. Tamaddoni Moghaddam, S.; Naimi-Jamal, M.R.; Rohlwing, A.; Hussein, F.B.; Abu-Zahra, N. High Removal Capacity of Arsenic from Drinking Water Using Modified Magnetic Polyurethane Foam Nanocomposites. *J. Polym. Environ.* **2019**, *27*, 1497–1504. [[CrossRef](#)]
67. Nguyen, T.K.; Li, X.; Ren, L.; Huang, Y.; Zhou, J.L. Polystyrene and low-density polyethylene pellets are less effective in arsenic adsorption than uncontaminated river sediment. *Environ. Sci. Pollut. Res.* **2023**, *30*, 95810–95827. [[CrossRef](#)] [[PubMed](#)]
68. Jin, L.; Chai, L.; Song, T.; Yang, W.; Wang, H. Preparation of magnetic Fe₃O₄@Cu/Ce microspheres for efficient catalytic oxidation co-adsorption of arsenic(III). *J. Cent. South Univ.* **2020**, *27*, 1176–1185. [[CrossRef](#)]
69. Gao, M.; Li, B.; Liu, J.; Hu, Y.; Cheng, H. Adsorption behavior and mechanism of modified Fe-based metal–organic framework for different kinds of arsenic pollutants. *J. Colloid Interface Sci.* **2024**, *654*, 426–436. [[CrossRef](#)]
70. Yao, S.; Jabeur, F.; Pontoni, L.; Mechri, S.; Jaouadi, B.; Sannino, F. Sustainable removal of arsenic from waters by adsorption on blue crab, *Portunus segnis* (Forskål, 1775) chitosan-based adsorbents. *Environ. Technol. Innov.* **2024**, *33*, 103491. [[CrossRef](#)]
71. Chu, W.; Zhang, Q.; Wu, B.; Zhou, H.; Li, F.; Cheng, Z.; Wu, J.; Yao, H.; Luo, G.; Yoriya, S.; et al. Adsorption of arsenic in flue gas in the wide temperature range of micron-sized flower like iron trioxide: Experiment and DFT. *Colloids Surf. Physicochem. Eng. Asp.* **2023**, *674*, 131956. [[CrossRef](#)]
72. Song, X.; Nong, L.; Zhang, Q.; Liu, J.; Zhang, S. Highly effective adsorption for both As(III) and As(V) in aqueous medium via magnetic chitosan-based composite microparticles: Low arsenic concentration, high column efficiency and adaptability. *J. Environ. Chem. Eng.* **2023**, *11*, 110874. [[CrossRef](#)]
73. Liudvinavičiute, D.; Rutkaite, R.; Bendoraitiene, J.; Klimavičiute, R.; Zambickaitė, G. Adsorption of caffeic acid on chitosan powder. *Polym. Bull.* **2021**, *78*, 2139–2154. [[CrossRef](#)]
74. Costa, L.F.; Ruotolo, L.A.M.; Ribeiro, L.S.; Pereira, M.C.; Camargo, E.R.; Nogueira, F.G.E. Low-cost magnetic activated carbon with excellent capacity for organic adsorption obtained by a novel synthesis route. *J. Environ. Chem. Eng.* **2021**, *9*, 105061. [[CrossRef](#)]
75. Cifuentes-Cabezas, M.; María Sanchez-Arévalo, C.; Antonio Mendoza-Roca, J.; Cinta Vincent-Vela, M.; Álvarez-Blanco, S. Recovery of phenolic compounds from olive oil washing wastewater by adsorption/desorption process. *Sep. Purif. Technol.* **2022**, *298*, 121562. [[CrossRef](#)]

76. Wang, M.; Tan, X.; Tu, Y.; Xiang, P.; Jiang, L.; Yang, A.; Xu, R.; Chen, X. Self-healing PDMS/SiO₂-CaCO₃ composite coating for highly efficient protection of building materials. *Mater. Lett.* **2020**, *265*, 127290. [[CrossRef](#)]
77. Alomayri, T. Performance evaluation of basalt fiber-reinforced geopolymer composites with various contents of nano CaCO₃. *Ceram. Int.* **2021**, *47*, 29949–29959. [[CrossRef](#)]
78. Alam, M.S.; Chowdhury, M.A. Characterization of epoxy composites reinforced with CaCO₃-Al₂O₃-MgO-TiO₂/CuO filler materials. *Alex. Eng. J.* **2020**, *59*, 4121–4137. [[CrossRef](#)]
79. Narayana Kota, S.; Alanka, S.; Lakshmipathi Raju, B. Mechanical characterization of nano-CaCO₃ inclusions reinforced PPS/GF polymer hybrid composites. *Mater. Today Proc.* **2023**. [[CrossRef](#)]
80. Echeverria, C.; Pahlevani, F.; Sahajwalla, V. Mechanical particle size reduction methods as potential interfacial optimization alternative for a low-carbon particulate reinforced marine bio-composite. *J. Clean. Prod.* **2019**, *221*, 509–525. [[CrossRef](#)]
81. Wang, S.; Li, J.; Li, F.; Li, J.; Zhang, C.; Ji, M.; Man, J.; Peng, S. Study on the influential effect of different CaCO₃ particle sizes on the internal pore structure of starch/fiber foaming composite materials. *Mater. Today Commun.* **2024**, *38*, 107867. [[CrossRef](#)]

Disclaimer/Publisher’s Note: The statements, opinions and data contained in all publications are solely those of the individual author(s) and contributor(s) and not of MDPI and/or the editor(s). MDPI and/or the editor(s) disclaim responsibility for any injury to people or property resulting from any ideas, methods, instructions or products referred to in the content.